Soft Matter

Thermal Transitions in Hydrated Layer-by-Layer Assemblies Observed Using Electrochemical Impedance Spectroscopy

Journal:	*Soft Matter*
Manuscript ID:	SM-ART-06-2014-001269.R1
Article Type:	Paper
Date Submitted by the Author:	01-Jul-2014
Complete List of Authors:	Sung, Choonghyun; Texas A&M University, Chemical Engineering Hearn, Katelin; Texas A&M University, Chemical Engineering Lutkenhaus, Jodie; Texas A&M University, Chemical Engineering

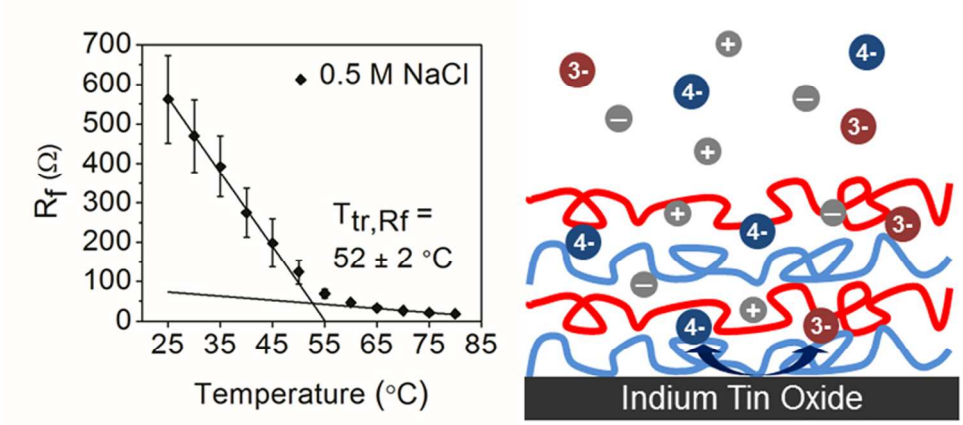

78x34mm (300 x 300 DPI)

Cite this: DOI: 10.1039/c0xx00000x

www.rsc.org/xxxxxx

ARTICLE TYPE

Thermal Transitions in Hydrated Layer-by-Layer Assemblies Observed Using Electrochemical Impedance Spectroscopy

Choonghyun Sung, Katelin Hearn and Jodie Lutkenhaus*

Received (in XXX, XXX) Xth XXXXXXXXX 20XX, Accepted Xth XXXXXXXXX 20XX

DOI: 10.1039/b000000x

Layer-by-layer (LbL) assemblies have been of great interest due to their versatile functionality and ease of fabrication, but their response to temperature is not completely understood. It has been recently shown that hydrated LbL assemblies of poly(diallyldimethylammonium chloride) (PDAC) and poly(styrene sulfonate) (PSS) under go a thermal transition much like a "glass-melt" transition. This thermal transition is of great interest because many LbL applications are found in water. Here, we report upon the nature of this thermal transition as probed using electrochemical impedance spectroscopy (EIS) as a function of assembly salt concentration, film thickness, and outermost layer. EIS reveals that the transition is signified by a structural rearrangement of virtual pores, resulting in increased conductivity and decreased surface coverage of the electrode. Two separate thermal transitions are obtained from changes in the film resistance ($T_{tr,Rf}$) and the charge transfer resistance ($T_{tr,Rct}$). Only $T_{tr,Rct}$ is strongly dependent on film thickness, salt concentration, and outermost layer, for which values ranging from 50 to 64 °C were observed. As the assembly salt concentration increases from 0.5 M to 1.0 M NaCl, $T_{tr,Rct}$ increases by about 10 °C. Below 20 layers, deviations of $T_{tr,Rct}$ with respect to outermost layer appear, in which PSS-capped LbL films tend to show elevated $T_{tr,Rct}$ values. These results suggest that extrinsic charge compensation plays a large role in the value of $T_{tr,Rct}$ in which a large degree of extrinsic charge compensation drives $T_{tr,Rct}$ towards higher values. On the other hand, $T_{tr,Rf}$ is largely unaffected by assembly parameters, and closer in value to prior reports via calorimetry and quartz crystal microbalance with dissipation.

Introduction

Layer-by-layer (LbL) assemblies offer immense promise for a variety of applications ranging from energy to life science.[1-3] These functional coatings and films are fabricated from the alternate adsorption of oppositely charged polyelectrolytes,[4] metallic or inorganic nanoparticles,[5, 6] and biological species,[7] for which structure and properties are modulated using assembly pH, salt concentration, and temperature.[8, 9] The sensitivity of an LbL film to assembly conditions as well as external stimuli can be attributed to the weak nature of non-covalent interactions (electrostatic, hydrogen bonding, van der Waals) existing between the two adsorbing species. As it will be shown here, temperature is a particularly intriguing parameter in that some LbL films respond dramatically in aqueous media. The reasoning behind this phenomenon is not well understood, and is explored herein using electrochemical impedance spectroscopy.

Understanding the nature of an LbL assembly's thermal transition in the hydrated state is of particular interest because many applications, such as drug delivery and separations, are found in aqueous media. For example, leveraging the thermal transition is crucial for temperature-responsive LbL films, capsules, and microtubes.[10-12] Further, it has been proposed that the mode of the film growth (linear *vs.* exponential) is influenced by the viscoelastic properties of film, which may be related to whether the film was assembled below or above its thermal transition temperature.[13, 14] The thermal transition itself has been clearly observed via atomic force microscopy (AFM) coupled with fluorescence microscopy,[15] calorimetry,[10, 11, 16] ^{2}H NMR spectroscopy,[16] and quartz crystal microbalance with dissipation (QCM-D).[14, 17] The majority of studies have focused upon a pair of strong polyelectrolytes, poly(diallyldimethylammonium chloride) (PDAC) and poly(styrenesulfonate) (PSS) assembled in the presence of salt.

For this LbL system, the thermal transition manifests as a reversible second-order thermal phenomena, yielding a response much like a glass transition. Upon heating through the transition, a significant drop in stiffness, an increase in viscoelasticity, and an increase in chain motion have been reported.[14-16] For this reason the thermal transition observed for the hydrated PDAC/PSS LbL system has been called a "glass-melt" transition, or simply a "glass transition", in prior literature. In light of our forthcoming publication, which contains simulations of the thermal transition, we now understand that the transition is related to the rearrangement of water molecules around ionic

groups on the polyelectrolyte, leading to enhanced polyelectrolyte mobility. This reasoning is supported by the observation that the same systems, when dry, do not have thermal transitions.[14, 18] Hydrated complexes also possess this transition, albeit at a lower temperature.[19]

Electrochemical impedance spectroscopy (EIS) has been widely used to study the interfacial and transport properties of polymer films, and offers new opportunities to assess the nature of thermal transitions in LbL assemblies. EIS has been used to monitor the swelling and shrinking of polymer hydrogels[20] and to investigate the chain conformation of polymer brushes.[21] LbL properties, such as permeability and swelling, have also been characterized using EIS for various pH values and salt concentrations.[22-24] EIS studies also provide a deeper understanding of LbL film structure and transport when investigated with the aid of a redox-active label, such as ferro/ferricyanide. It has been proposed that the redox probes hop between "reluctant" exchange sites within the LbL film.[25, 26] Pardo-Yissar *et al.* showed that Donnan inclusion and Donnan exclusion strongly affected the charge transfer resistance. When the charge of the redox active probe matched that of the film's outermost layer, Donnan exclusion occurred and the charge transfer resistance increased. Conversely, for the case of opposite charge, Donnan inclusion occurred, and the charge transfer resistance was negligible, consistent with a neutralized porous film structure.[23] Barreira *et al.* suggested sophisticated models for the impedance response, considering an inhomogeneous LbL film structure characterized by spots or capillaries at the electrode-film interface where electrochemical transport is favored.[24]

Temperature-controlled EIS studies on LbL assemblies are relatively rare. Silva *et al.* investigated thermal behavior over a limited temperature range (15 to 45 °C) for polyallylamine/PSS LbL assemblies.[27] It was reported that the diffusion coefficient increased and film resistance decreased with increasing temperature, but no thermal transition was observed, possibly because of the limited temperature range investigated. Elsewhere, Alonso-Garcia *et al.* measured the glass transition temperature of grafted polyelectrolyte brushes using temperature-controlled EIS.[28] The glass transition temperature of the brushes coincided with a discontinuity in the charge transfer resistance and diffusion coefficient with respect to temperature. Motivated by these results, we hypothesized that LbL films would show distinct variations in electrochemical behavior associated with a thermal transition via EIS.

In this work, we study the structure of PDAC/PSS LbL assemblies in aqueous media as a function of temperature using EIS with a redox-active probe. The effect of assembly salt concentration, film thickness, and identity of the outermost layer on the thermal transition temperature is investigated. A modified Randles circuit is used to quantitatively analyze the impedance spectra in terms of charge transfer resistance, capacitance, and Warburg impedance. It is found that some circuit elements are particularly responsive to temperature, which is interpreted in the context of the nature of the thermal transition. To our knowledge, this is the first report of temperature-controlled EIS in which the thermal transition of PDAC/PSS LbL assemblies is demonstrated. EIS is particularly powerful in that it allows one to probe the structure of the film itself at a variety of frequencies and time scales.

Experimental section

Materials. Poly(diallyldimethylammonium chloride) (PDAC, Mw =350,000 g/mol) and poly(styrene sulfonate salt) (PSS, Mw= 500,000 g/mol) were purchased from Sigma Aldrich. Indium-tin oxide (ITO) coated glass was purchased from Delta Technologies. Potassium hexacyanoferrate(II) trihydrate ($K_4[Fe(CN)_6]\cdot 3H_2O$) and potassium ferricyanide(III) ($K_3[Fe(CN)_6]$) were purchased from Alfa Aesar and Sigma Aldrich, respectively.

Preparation of layer-by-layer assemblies. PDAC/PSS LbL assemblies were prepared on ITO- coated glass using a programmable slide stainer (HMS series, Carl Zeiss Inc.). ITO-coated glass was cleaned by immersion in a water/NH_4OH/H_2O_2 (5:1:1) mixture at 70°C for 15 min followed by plasma-cleaning for 5 min. ITO-coated glass slides were immersed in PDAC solution for 15 min followed by three rinses with 18.2 MΩ·cm water for 2, 1, and 1 min. Then, the substrates were immersed in PSS solution for 15 min, followed by three water rinses as before. The cycle was repeated n times to form a $(PDAC/PSS)_n$ LbL film in which the subscript describes the number of layer pairs. The polymer solution's concentration was fixed at 1 mg/ml. Two NaCl concentrations, 0.5 M and 1.0 M, were used in this study for both water rinse baths and polyelectrolyte solutions. These adsorption processes were repeated as desired. The LbL films were dried in a convection oven at 70 °C for 15 min, and stored in a sealed vial until further use.

Electrochemical characterization. Electrochemical impedance measurements were performed in a standard three-electrode cell using Ag/AgCl (4M KCl) as the reference electrode (Pine Research Instrumentation) and platinum wire of 0.3 mm diameter (Alfa Aesar) as the counter electrode. LbL-coated, ITO-coated glass slides were used as working electrodes (Delta Technologies). The active area of the working electrode immersed in supporting electrolyte was 2.1 cm^2. The supporting electrolyte was an aqueous solution of NaCl in which the concentration was matched to that used for assembly to avoid the possibility of salt annealing. In the case of bare ITO, the NaCl concentration was 0.5 M. $K_3[Fe(CN)_6]$ and $K_4[Fe(CN)_6]$ (5 mM each) were used as redox-active probes. The electrochemical cell was held at 25 °C and purged with nitrogen for 30 min. Impedance measurements (Solartron 1287) were performed every 5 °C up to 80 °C after being held isothermally at a given temperature for 15 min under nitrogen purge. The DC potential was set to the open circuit potential and the AC amplitude was 10 mV. Frequency was scanned from 10^4 Hz to 0.02 Hz. Impedance data were modeled using commercial software (Zview, Scribner Associates, Inc.), which uses a complex nonlinear least squares fitting method. EIS measurements were done for three separate samples at a given condition, and the error was taken as the standard deviation.

UV-Vis spectroscopy. LbL films on the quartz cuvette slides were immersed in supporting electrolyte similar to that used for EIS measurements. UV spectra were obtained (Hitachi U-4100) at an absorbance of 226 nm to monitor the relative amount of PSS.[29]

Surface morphology and film thickness. Surface morphologies

of PDAC/PSS LbL films were investigated using atomic force microscopy (AFM) (Dimension Icon AFM, Bruker Corporation). Measurements were performed in tapping mode under dry conditions at a scan rate of 1.0 Hz. LbL film thickness was measured using profilometery (D-100, KLA Tencor) and/or ellipsometry (LSE stokes, Gaertner) after drying the samples at 65 °C for 30 min. Three separate samples were used for the thickness measurements, and standard deviation was taken as the error.

Results and discussion

Figure 1 shows typical electrochemical impedance spectra in the form of Nyquist diagrams for ITO electrodes with and without PDAC/PSS LbL coatings at varying temperatures. Bode plots are given in Figure S1, ESI. LbL films made at 0.5 and at 1.0 M NaCl were explored; we also attempted to evaluate films made without salt, but we encountered issues associated with salt annealing during exposure to the aqueous electrolyte to which some salt is necessary for the measurement. The Nyquist plots for the LbL-coated electrodes show semicircles in the high frequency region and, for higher temperatures, a roughly 45° straight line in the low frequency region associated with a Warburg impedance (semi-infinite diffusion). On the other hand, for the bare ITO electrode, only a single 45° straight line was observed. It is clear that the appearance of semicircles in the Nyquist plots is due to the presence of the LbL film.

For PDAC/PSS LbL films assembled at 0.5 M NaCl, the semicircle's diameter decreased and became skewed as the temperature increased (Figure 1a). At room temperature, the semicircle was nearly perfect in semicircular shape, but the skewedness became distinct at 75 °C as shown in the inset of Figure 1a. A Warburg impedance was not clearly detected at low temperatures, indicating kinetic control, but as the temperature increased a Warburg impedance appeared, indicative of facile kinetics and diffusion control.[30]

As for the impedance spectra of PDAC/PSS LbL films assembled at 1.0 M NaCl, the semicircle's diameter also decreased with increasing temperature (Figure 1b). Compared to the LbL films assembled at 0.5 M NaCl, the PDAC/PSS LbL films assembled at 1.0 M NaCl showed much smaller semicircles even for comparable thicknesses. There was a clear Warburg impedance even at room temperature for LbL films assembled at 1.0 M NaCl. We also observed skewing at high temperatures as before.

In order to analyze the electrochemical properties quantitatively, the impedance spectra were fitted to a modified Randles equivalent circuit (Figure 2). This equivalent circuit has been widely used to model electrodes modified with LbL assemblies,[31-33] polymer films,[34] and polymer brushes.[35, 36] R_s is the solution resistance, and R_f represents the pore resistance of the film.[34] "CPE" stands for constant phase element and represents the non-ideal capacitive behavior of the film. The CPE is frequently used in place of an ideal capacitor to consider depressed semi-circles or non-vertical lines in the low-frequency regions of Nyquist plots.[37] The impedance of a CPE is expressed as $Z = 1/[T(j\omega)^p]$, where j is square root of -1, T is the admittance (CPE-T), and p is an adjustable exponent (CPE-P).[37] When p = 1, the CPE becomes an ideal capacitor. For 0.5 < p < 1, the film is interpreted as being either porous and rough or as having a non-uniform distribution of current. R_{ct} is charge transfer resistance,

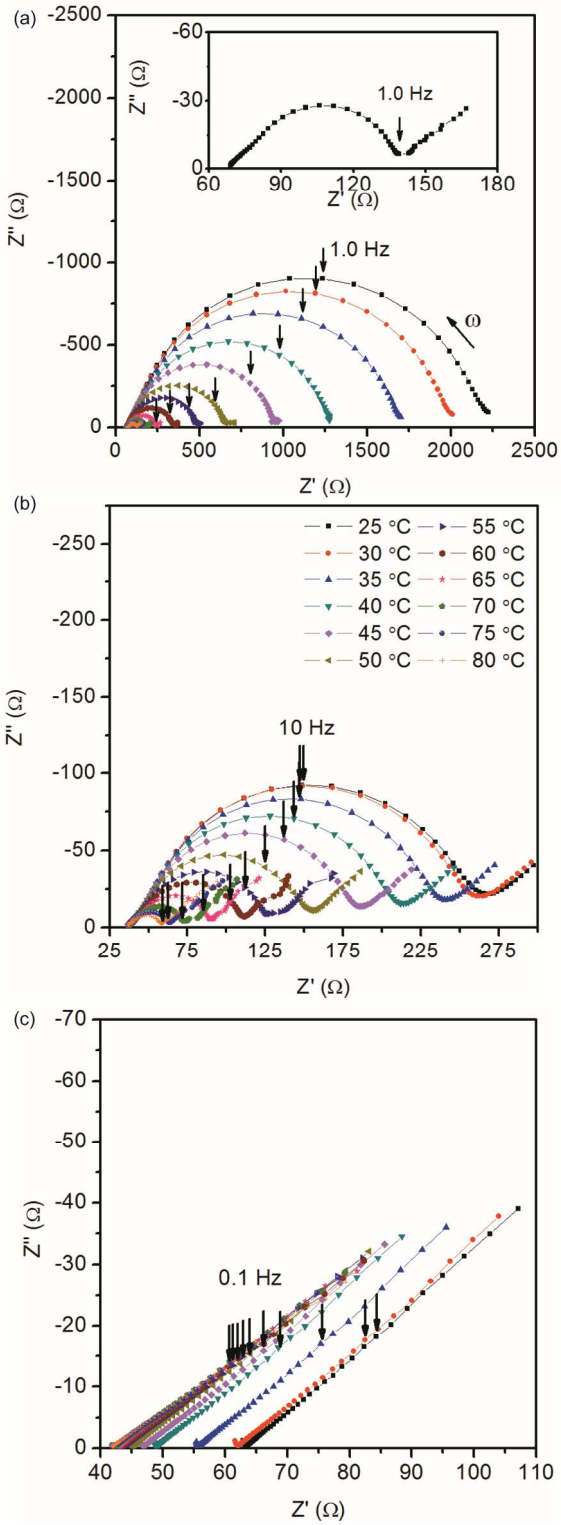

Fig 1. Nyquist plots of electrochemical impedance spectra taken at different temperatures for an ITO electrode modified with (a) $(PDAC/PSS)_{11}$ assembled at 0.5 M NaCl (~100 nm) and (b) $(PDAC/PSS)_7$ assembled at 1.0 M NaCl (~125 nm), as well as (c) an unmodified ITO electrode. The inset of Figure 1a is the magnification of the impedance response measured at 75 °C for $(PDAC/PSS)_{11}$ assembled at 0.5 M NaCl. The legend in (b) applies to all panels. Solid lines are provided to guide

the eye. The electrolyte consisted of NaCl in water, in which the concentration of NaCl was matched to the assembly conditions so as to minimize salt annealing.

C_{dl} is double layer capacitance, and Z_w is a Warburg impedance associated with semi-infinite linear diffusion. Figure 3 shows typical impedance spectra fitted with the modified Randles equivalent circuit for low and high temperatures. Skewedness in the high frequency region is fit very well by this model, as shown in Figure 3b.

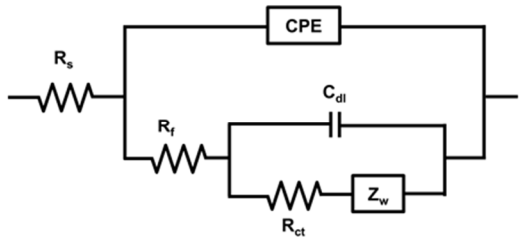

Fig. 2 Modified Randles equivalent circuit used to model electrochemical impedance spectra, where R_s is the solution resistance, R_f is film resistance, CPE is the constant phase element of the film, R_{ct} is charge transfer resistance, C_{dl} is double layer capacitance, and Z_w is Warburg impedance.

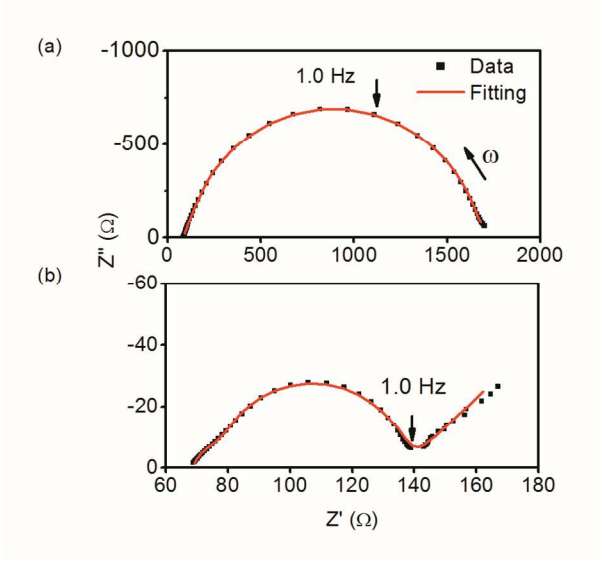

Fig. 3 Nyquist plots taken at (a) 35 and (b) 75 °C for ITO electrodes modified with $(PDAC/PSS)_{11}$ LbL films assembled at 0.5 M NaCl. Black dots represent experimental data, and the red line represents the equivalent circuit model.

Plots of film resistance (R_f) vs. temperature for LbL films assembled at 0.5 M and 1.0 M NaCl are shown in Figure 4. R_f generally decreased in two distinct modes upon heating. In the first mode, R_f decreased rapidly upon heating from room temperature. In the second mode, R_f decreased only slightly above 55 °C. The transition temperature ($T_{tr,Rf}$) was obtained from the intersection of two lines extrapolated from low and high temperature regions. Both LbL films assembled at 0.5 M and 1.0 M NaCl displayed transition temperatures (52 ± 2 °C and 54 ± 1°C, respectively) close to those measured in our previous study using QCM-D and modulated differential scanning calorimetry (51.0 ± 0.2 °C and 52 ± 1°C, respectively).[14] We have found that the shape of the R_f-T curve is similar for all cases investigated herein except for one notable exception: PDAC/PSS LbL films assembled at 1.0 M NaCl for thicknesses below 100 nm. In that case, R_f decreased linearly with temperature and no clear transition was observed. This observation is consistent with that of a patchy film in which the electrode is not fully covered.

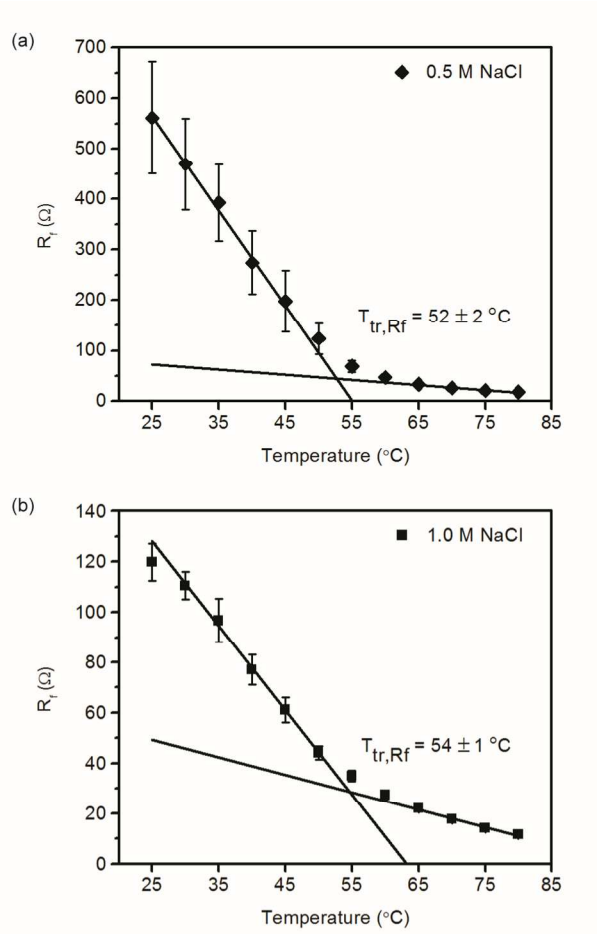

Fig. 4 Film resistance (R_f) as a function of temperature for (a) $(PDAC/PSS)_{11}$ LbL film assembled at 0.5 M NaCl (~100 nm) and (b) $(PDAC/PSS)_9$ LbL film assembled at 1.0 M NaCl (~225 nm). R_f was obtained from application of the equivalent circuit shown in Figure 2 to impedance spectra such as those shown in Figure 1. Error bars represent the standard deviation of three separate samples. PSS is the outermost layer.

R_f has been interpreted as the resistance resulting from the penetration of electrolyte through real and virtual pores within the film.[34, 36] R_f is related to the thickness of the film t, the conductivity of the film swollen with electrolyte κ and the cross sectional area by Equation 1.

$$R_f = \frac{t}{\kappa A_c} \quad (1)$$

The steady decrease in R_f with increasing temperature suggests

that the film decreases in thickness and/or the conductivity of the film increases. From prior QCM-D measurements, deswelling occurred over a range of 35-50 °C when PSS was the outermost layer, which does not fully explain the decrease in R_f over the full range herein. Therefore, an increase in conductivity of ions through the film must be the major contributing factor for R_f's decrease with increasing temperature. Because transport of monovalent ions is less susceptible to Donnan exclusion compared to multivalent ions or heavily charged electroactive ions such as ferrocyanide/ferricyanide redox couple,[30, 38] it can be concluded that the conductivity mainly arises from ions from the supporting electrolyte and not the redox-active probe.

Considering the inverse relationship between conductivity and R_f, Figure 4 can be recast as a steady increase in conductivity from room temperature up to $T_{tr,Rf}$, and then a marginal increase for higher temperatures. Conductivity is closely tied to the structure of the film, such as the shape and occurrence of electrolyte-filled virtual pores through which ions travel as well as the extent of extrinsically compensated sites reserved for ion transport via "hopping". Upon comparison with other investigations, the former likely dominates the temperature-conductivity response. For instance, the stiffness of PDAC/PSS LbL capsules in water decreased fairly linearly until 45 °C and leveled off,[15] in which a transition from a glassy to a viscous fluid state was suggested. Our forthcoming work shows through simulations that the transition is related to the dehydration of ionic groups along the polyelectrolyte and an increase in polyelectrolyte chain mobility. Such an increase in mobility could be responsible for a restructuring of the film and the virtual pores therein. Also, simulations show no discernable change in the ratio of extrinsic to intrinsic charge compensation above or below the transition.

Given the preceding observations regarding R_f, we next turn to the interpretation of R_{ct}. R_{ct} represents the charge transfer associated with executing the redox reaction, and is, thus, directly related to the redox probe and its state within or just outside the film. Silva *et al.* proposed that in early stages of LbL growth, the surface is patchy and the apparent R_{ct} is strongly tied to the active area of the partially blocked electrode.[27] As the number of layers increases, a homogeneous membrane is eventually achieved for which partitioning of the redox active probe becomes important.[24, 30, 39] Here, we chose to account for both surface coverage and partitioning because our films possess a loose network (which contributes to virtual pores) and because our films are relatively thick (which allows for some partitioning). The partition coefficient K of the redox active probe in the film *vs.* the bulk solution and the surface coverage θ are related to the observed R_{ct} by the following equation[27]:

$$R_{ct} = \frac{R_{ct,bare}}{K(1-\theta)} \qquad (2)$$

where $R_{ct,bare}$ is the charge transfer resistance of the electrode in the absence of the LbL film. For the ferro/ferricyanide redox couple on bare ITO, R_{ct} = 17.63 Ω cm^2 at 298 K,[40] which would correspond to 37 Ω for our active area of 2.1 cm^2.

Figure 5a shows the charge transfer resistance as a function of temperature for the PSS-terminated LbL films assembled at 0.5 M NaCl. At room temperature, R_{ct} is over 50 times higher than $R_{ct,bare}$, which suggests strong partitioning and/or high surface coverage. R_{ct} decreases rapidly as temperature increases and then levels off at high temperatures as similar to the results of R_f vs. temperature. Using a similar procedure as before with R_f, the transition temperature from the R_{ct}-T plots ($T_{tr,Rct}$) was 54.0 +/- 0.8 °C. From Eqn. 2, the decrease in R_{ct} can be interpreted as either an increase in the partition coefficient or a decrease in the surface coverage of the film. The former is less likely because it has been shown that ferricyanide concentration in the film decreases (*i.e.,* K decreases) with increasing temperature.[41] Therefore, we propose that the temperature-dependent behavior of R_{ct} is dominated by the surface coverage of the electrode. Above the $T_{tr,Rct}$, the marginal decrease in R_{ct} suggests that the film is highly permeable to the redox active probe, and perhaps is brought about by an increase in polyelectrolyte mobility and structural rearrangement, leading to a very low surface coverage. In the limiting case of a highly porous or mobile LbL coating, K would approach unity, θ would approach a small finite value, and R_{ct} would approach that of the bare electrode. This situation is perhaps achieved at high temperatures when R_{ct} is fairly low, Figure 5a.

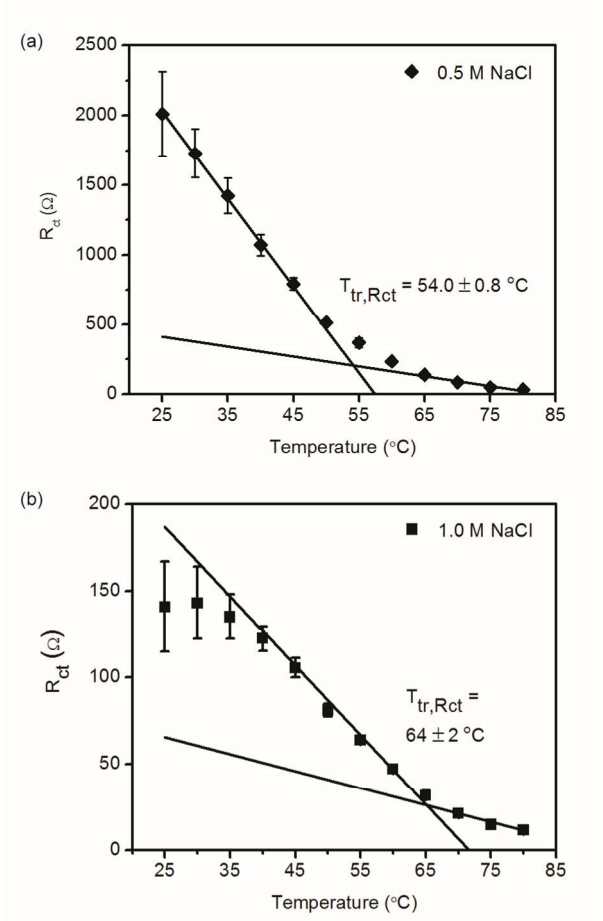

Fig. 5 Charge transfer resistance (R_{ct}) as a function of temperature for (a) $(PDAC/PSS)_{11}$ LbL films assembled at 0.5 M (~100 nm) and (b) $(PDAC/PSS)_7$ assembled at 1.0 M NaCl (~125 nm). R_{ct} was obtained from application of the equivalent circuit shown in Figure 2 to impedance spectra such as those shown in Figure 1. PSS is the outermost layer.

On the other hand, for the LbL film assembled at 1.0 M NaCl, a sigmoidal shape is observed (Figure 5b). R_{ct} declines rapidly starting at 36 °C, and then decreases slightly beyond 64 °C. This sigmoidal shape was observed for both PDAC- and PSS-terminated LbL films assembled at 1.0 M NaCl, and for PSS-terminated LbL films assembled at 0.5 M NaCl of just a few layer pairs. It can be inferred that the sigmoidal shape tends to appear for films in which coverage is patchy (0.5 M NaCl of just a few layers) or in which the structure has a high degree of extrinsic charge compensation (1.0 M NaCl). Several competing phenomena are perhaps responsible for this shape. Firstly, an increase in temperature could lead to a decrease in surface coverage and a decrease in R_{ct} as chains gain more mobility. Secondly (and mentioned previously), the partition coefficient of the redox active label is expected to decrease with increasing temperature, which would lead to an increase in R_{ct}. Thirdly, $R_{ct,bare}$ is expected to decrease with temperature, causing an decrease in the observed R_{ct}; however, inspection of Figure 1c shows that any change in $R_{ct,bare}$ is negligible as compared to changes displayed in Figure 5.

Upon comparison, R_{ct} was generally much higher for the LbL-coated electrode assembled at 0.5 M NaCl *vs.* 1.0 M NaCl. This result is easily rationalized by considering the structure of the PDAC/PSS LbL film as a function of ionic strength of assembly. Films assembled at higher salt concentrations have more extrinsic charge compensation and form a looser network,[42] which offers decreased surface coverage and lower R_{ct}.

The constant phase element, representing the non-ideal capacitance of the LbL film, was studied as a function of temperature (Figure S2, ESI). From room temperature to about 55 °C, CPE-P (where CPE-P = p) remained constant at about 0.9, and above 55 °C, CPE-P decreased strongly with temperature. CPE-P is related to surface roughness, water permeation, or the interaction and mobility of polarizable groups. CPE-P generally decreases from 1.0 to 0.5 as the roughness or porosity increases.[37] In corrosion studies of polymer-coated metals, it was shown that CPE-P generally decreases as polymer degradation proceeds due to water permeation into the film.[43, 44] It is also possible that CPE-P decreases as the interaction and mobility of polarizable groups increases.[45] As it will be shown later, the roughness of the LbL films actually decreased when the films were annealed in supporting electrolyte at a high temperature. Thus, it is more plausible that the decrease of CPE-P with temperature is linked to an increase in mobility of polyelectrolyte chains. CPE-T was also analyzed, but no clear temperature dependence was observed as compared to CPE-P.

Double layer capacitance (C_{dl}) was also studied as a function of temperature (Figure S3, ESI). According to the classical double layer model, C_{dl} should decrease with temperature.[46, 47] However, in this study, C_{dl} was fairly constant at low temperatures, and increased slightly above 55 °C. The slight increase might be related to an increase in internal surface area owing to the formation of new virtual pores.

The Warburg impedance, which arises from diffusion of redox active probes through the film, was analyzed as a function of temperature. The apparent diffusion coefficient of the redox couple can be calculated from the Warburg impedance according to the following equation,[48]

$$D = \left(\frac{\sqrt{2}RT}{n^2F^2A\sigma C_{bulk}}\right)^2 \quad (3)$$

where, n is the number of electrons transferred, F is Faraday's constant, A is the electrode area, R is the gas constant, T is absolute temperature, σ is a Warburg parameter, and C_{bulk} is the concentration of the redox probe in bulk solution. The diffusion coefficient for LbL films assembled at 1.0 M NaCl was obtained for all temperatures investigated, but for LbL films assembled at 0.5 M NaCl the diffusion coefficient could only be obtained above 50 °C due to the absence of a Warburg impedance at lower temperatures (Figure S4, ESI).

The diffusion coefficient for LbL films assembled at 1.0 M NaCl increased fairly linearly with temperature without any apparent thermal transition and was in the range of 5 x 10^{-6} – 1.5 x 10^{-5} cm^2/s. For bare ITO, we calculated a comparable diffusion coefficient around 10^{-6} – 10^{-5} cm^2/s, consistent with previous literature.[49] This value is much higher than that reported from rotating disc electrode measurements, 10^{-10} – 10^{-9} cm^2/s, in which "reluctant" ion exchange was proposed.[25, 41] Therefore, the diffusion coefficients measured here could represent the diffusion of redox active probes through virtual pores or bulk diffusion from the solution because the values are closer to that of bulk electrolyte. The former possibility can be eliminated considering that the concentration of the redox active probe decreases as a function of temperature, so one would expect to see a decrease in D according to Eqn 3. Thus, the diffusion coefficients in Figure S4 likely arise from bulk diffusion from the electrolyte to the film.

The transition temperatures were investigated as a function of film thickness and salt concentration. Figure 6a and b show $T_{tr,Rf}$ and $T_{tr,Rct}$, respectively, for films assembled at 0.5 M and 1.0 M NaCl. It is important to note that $T_{tr,Rf}$ and $T_{tr,Rct}$ are not always identical because they probe separate phenomena. $T_{tr,Rf}$ comes from the resistance of the film, which is swollen with electrolyte, and $T_{tr,Rct}$ comes from the charge transfer resistance associated with redox active probes in the film. In other words, $T_{tr,Rf}$ reports the state of electrolyte in the film, and $T_{tr,Rct}$ probes the state of the redox active probe in the film.

In Figure 6a, the $T_{tr,Rf}$ of LbL films assembled at 0.5 M NaCl is around 52.0 ± 0.4 °C for all thicknesses, except for ~25 nm film, which shows a slightly lower $T_{tr,Rf}$ of 49.4 ± 0.4°C. For LbL films assembled at 1.0 M NaCl, $T_{tr,Rf}$ remained fairly constant with thickness, having an average value of 54.9 ± 0.4°C. For films assembled at 1.0 M NaCl we did not observe any discernable transitions for thicknesses below 125 nm, perhaps because of patchy growth. There appears to be a lack of strong thickness dependence for $T_{tr,Rf}$, which suggests that the state of the electrolyte in the film does not vary with significantly over the thickness range investigated.

The dependence of assembly salt concentration on $T_{tr,Rct}$, on the other hand, is strikingly different, Figure 6b. As described earlier, plots of R_{ct} vs. temperature showed one transition for the films assembled at 0.5 M NaCl and a sigmoidal shape with two transitions for those assembled at 1.0 M NaCl, the higher of which is plotted in Figure 6b. For the LbL films assembled at 0.5 M NaCl, $T_{tr,Rct}$ increases from 50.4 ± 0.6 °C to 61 ± 1 °C as film thickness decreases from 300 nm to 25 nm. For the LbL films

assembled at 1.0 M NaCl, $T_{tr,Rct}$ increases from 58.8 ± 0.3 °C to 64 ± 2 °C as film thickness decreases from 525 nm 125 nm. On average, the $T_{tr,Rct}$ of the LbL film assembled at 1.0 M is about 11 °C higher compared to the films assembled at 0.5 M NaCl at the equivalent thickness. The elevated transition temperatures for films assembled at 1.0 M NaCl may be explained in the context of extrinsic charge compensation. Films assembled at 1.0 M NaCl have a higher degree of extrinsic charge compensation, which provides more sites for interaction with (or trapping of) multivalent ferrocyanide and ferricyanide ions. Thus, higher temperatures are needed to undergo the transition.

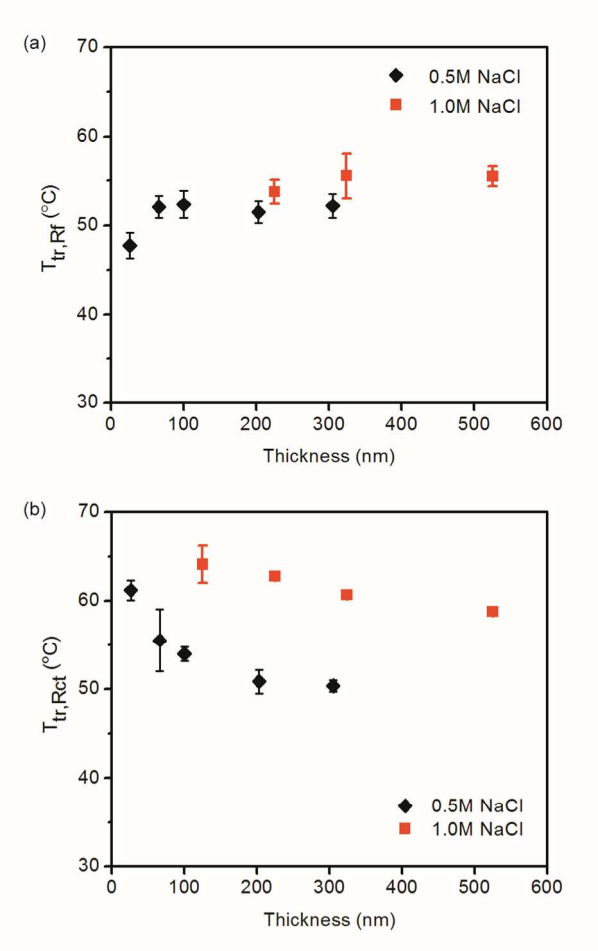

Fig. 6 (a) The transition temperature ($T_{tr,Rf}$) obtained from plots of R_f vs. temperature, and (b) the transition temperature ($T_{tr,Rct}$) obtained from plots of R_{ct} vs. temperature as a function of film thickness and salt concentration for PSS-terminated LbL films.

We next turn to the influence of the outermost layer, which for some LbL systems, strongly affects electrochemical properties via Donnan inclusion and exclusion.[23-25, 30] For example, an odd-even effect was previously observed via rotating disc electrode experiments, in which Donnan inclusion was shown to increase the local concentration of redox active probes at the film's surface.[25] To understand the effect of the outermost layer, $T_{tr,Rf}$ and $T_{tr,Rct}$ were obtained for LbL films terminated with either PSS or PDAC, Figure 7. For comparison, a plot of thickness vs. number of layers is shown in Figure S5. For $T_{tr,Rf}$ there is no clear difference between the different terminating layers, which is consistent with the idea that $T_{tr,Rf}$ depends on the conductivity of the film swollen with electrolyte, Figure 7a. Had the $T_{tr,Rf}$ been dependent on the multivalent redox probe, a strong odd-even effect would have been apparent. $T_{tr,Rf}$ was fairly constant for 20-50 layers, whereas it decreased slightly below 12 layers, which is about 25 nm in thickness. It has been previously shown that water content in PDAC/PSS LbL films increased from 35% to 65% as the number of layers pairs decreased from 7 to 1,[50] for which water acts as a plasticizer and perhaps lowers the film's $T_{tr.}$ It is also possible that the change in polymer composition or ion-pairing density might have taken place in 25 nm films.

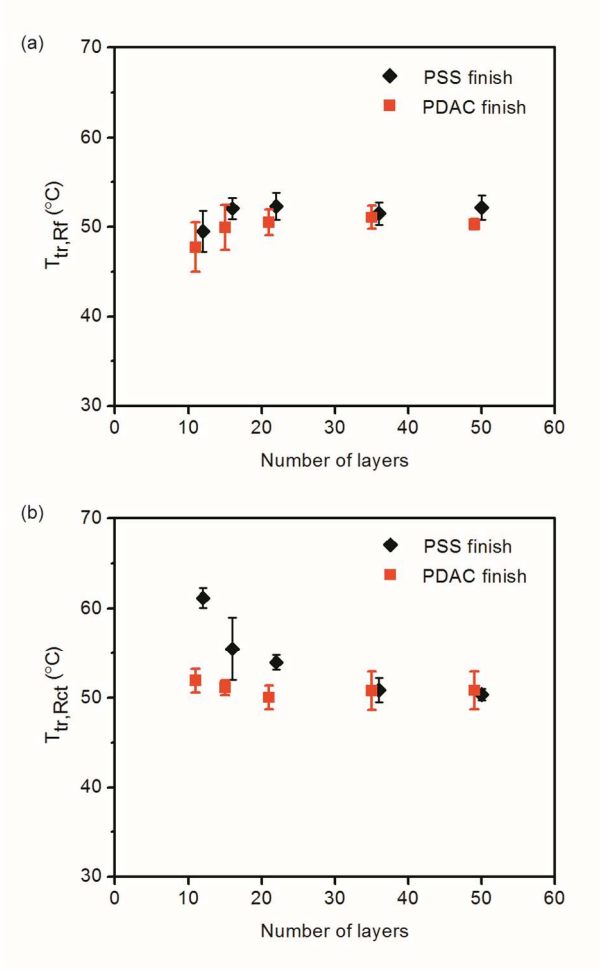

Fig. 7(a) The transition temperature (Ttr,Rf) obtained from plots of Rf vs. temperature, and (b) the transition temperature (Ttr,Rct) obtained from the plots of Rct vs. temperature as a function of film thickness and outermost layer for LbL films assembled at 0.5 M NaCl concentration.

On the other hand, the outermost layer strongly affects $T_{tr,Rct}$, especially for films of 20 layers or less, Figure 7b. Above 20 layers, $T_{tr,Rct}$ is around 50 °C for both PDAC- and PSS-terminated films. However, the $T_{tr,Rct}$ for PSS-terminated films increases about 10 °C as the number of layers decreases below 20, whereas $T_{tr,Rct}$ remains relatively constant for PDAC-terminated films. One might be tempted to claim that Donnan exclusion of ferro/ferricyanide via PSS is driving the $T_{tr,Rct}$ towards higher

temperatures, but a recent study from Ghostine *et al.*[42] indicates that Donnan exclusion can be largely discounted. Beyond a critical number of layer pairs, a reservoir of PDAC builds up within the film, and the net charge is positive regardless of the outermost layer. In this regard, Donnan *inclusion* perhaps becomes the norm for the PDAC/PSS LbL film beyond 20 layers, as evidenced by $T_{tr,Rct}$'s lack of dependence on outermost layer. Below this critical number of layers, the film's net charge flips between positive and neutral,[42] for which the redox active probes alternate between experiencing Donnan inclusion or lack thereof when PDAC or PSS are outermost layers, respectively. It has been suggested[42] that below this critical number of layer pairs the film exists as a glassy stoichiometric complex when PSS is the outermost layer and becomes rubbery when PDAC is outermost. This observation is consistent with the elevated $T_{tr,Rct}$'s for PSS-capped LbL films.

At room temperature, the outermost layer also affects the absolute values of R_{ct} and R_f, which are both higher when PDAC is the outermost (odd) layer are shown in Figure 8. R_f is only slightly affected, which supports the supposition that R_f is related to the resistance of the porous electrolyte-swollen film. R_{ct}, on the other hand, is higher in magnitude and strongly sensitive to outermost layer. This might be rationalized by assuming some dependence of partitioning or surface coverage on the outermost layer, in which PDAC-terminated films perhaps might have decreased K and increased θ. However, the surface coverage is not expected to change strongly based on the outermost layer, so, by elimination, partitioning is likely to dominate. The upwards oscillation of R_{ct} for both PDAC and PSS outermost layers is very similar in trend to the quantity of extrinsic charge, as reported by Ghostine et al.[42] This observation supports the idea that R_{ct} is related to the state of the redox active probe, whose transport is linked to the number of extrinsic sites. It is possible that a large degree of extrinsic compensation slows transport as multiple extrinsic polyelectrolyte sites perhaps trap redox active probes, thus affecting partitioning. This idea is contrary to Donnan inclusion,[23, 51] and has been suggested elsewhere.[24] Had Donnan inclusion dominated, one would have observed consistently lower R_{ct} values for PDAC- capped films, contrary to our findings; therefore we conclude that the extent of extrinsic charge compensation dominates R_{ct}.

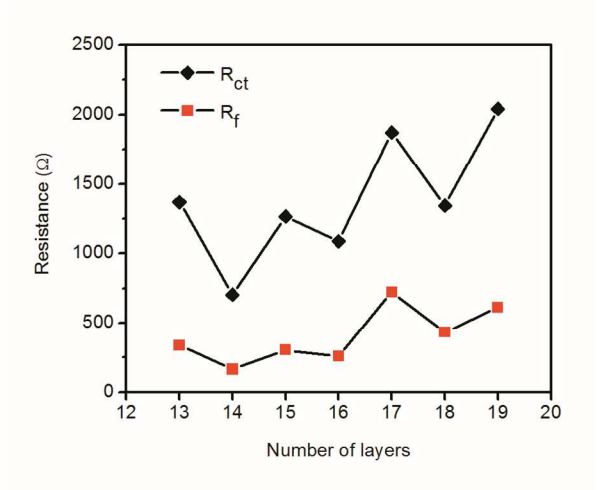

Fig. 8 R_f and R_{ct} as a function of layers for LbL films assembled at 0.5 M NaCl, evaluated at 25 °C. Odd numbers corresponds to PDAC layers, and even numbers corresponds to PSS layers.

It has been reported that PDAC/PSS LbL films dissolve at high salt concentrations,[52] and there is concern that the LbL film will disassemble in water at high temperatures.[10, 53] To monitor this possibility, an LbL-coated quartz substrate was annealed in the same supporting electrolyte used in EIS measurements at varying temperatures. UV absorbance at a wavelength of 225 nm, which is characteristic of PSS, was measured and scaled against the UV absorbance at room temperature,[54] (Figure S6 and S7, ESI). The film retained 94 % of its PSS, even when incubated at 80 °C, and dry film thickness decreased by only about 2 %. Therefore, disassembly during the course of EIS measurements is of minor concern. The dry film thickness also decreased by 2% (Figure S8, ESI).

The surface morphologies of the LbL films were also investigated before and after EIS measurements (Figure 9). Prior to EIS measurements, the as-made LbL film exhibited a well-known vermiculate surface morphology[55] with a root mean square (RMS) roughness of 7.5 nm (Figure 9a). However, after EIS up to 80 °C, the vermiculate surface morphology disappeared, and the film became fairly smooth (RMS roughness, 1.3 nm) (Figure 9b). Smoothing of LbL films due to salt annealing at room temperature is a well-known phenomena.[56, 57] However, annealing of LbL films at high temperature has not been reported to our knowledge. To verify whether this is due to the temperature, time, or electrical effects during EIS measurements, we annealed the film in a supporting electrolyte without applying electric field at 25 °C for 7 hours, which is the same period LbL films are immersed during EIS measurements, and at 80 °C for 30 min. After annealing at 25 °C for 7 hours, the vermiculate structure is still observed (RMS roughness, 10.5 nm) (Figure 9c). On the contrary, the film surface becomes fairly smooth (RMS roughness, 2.5 nm) when annealed at 80 °C for 30 min (Figure 9d). These results imply that the surface morphology

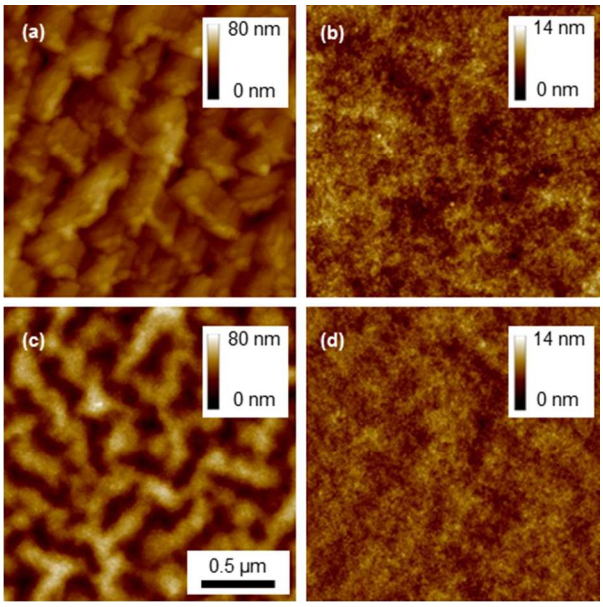

Fig. 9 AFM topographic images of $(PDAC/PSS)_{11}$ LbL films assembled at 0.5 M NaCl (a) as-made, (b) after EIS measurement, and after annealing in supporting electrolyte (c) at 25 °C for 7 hours and (d) at 80 °C for 30 min.

changes are mainly driven by temperature rather than time or electrical effects.

Conclusions

Thermal transitions for hydrated PDAC/PSS LbL films were studied using electrochemical impedance spectroscopy with ferrocyanide/ferricyanide as a redox active probe for the first time. Thin films (less than 10 layers) behave as patchy coatings, for which diffusion through the film is similar to bulk electrolyte. Thicker films (greater than 10 layers) exhibit thermal transitions that arise from changes in the film's resistance ($T_{tr,Rf}$) and the charge transfer resistance ($T_{tr,Rct}$). These transitions are not necessarily the same because they arise from different phenomena, as elaborated below.

$T_{tr,Rf}$ is related to the state of the film swollen with electrolyte and the film's network of virtual pores. The $T_{tr,Rf}$ values observed herein coincide with those observed elsewhere via QCM-D and calorimetry,[14] and were largely independent of thickness, outermost layer, and salt concentration. These results indicate that the transition is tied to a structural rearrangement of the LbL film, resulting in increased conductivity through the film.

$T_{tr,Rct}$ is related to the state of the redox active probe near and within the LbL film. Upon going through the transition, the charge transfer decreases and then levels off, suggestive of a net decrease in surface coverage towards a finite value. The $T_{tr,Rf}$ values observed herein are strongly dependent on thickness, outermost layer, and salt concentration. As the number of layers decreased, the identity of the outermost layer began to dominate, for which $T_{tr,Rct}$ was at most 10°C higher for PSS-capped films. Further, as the ionic strength of assembly increased from 0.5 M to 1.0 M NaCl, $T_{tr,Rct}$ was consistently about 10°C higher as well. These results indicate that extrinsic charge compensation plays a large role on the value $T_{tr,Rct}$, for which a higher extent of extrinsic charge compensation drives $T_{tr,Rct}$ towards higher values. This is suggestive of trapping of the negatively charged redox ion probe in pockets of unpaired positively charged PDAC segments. Donnan inclusion was also considered, but determined not to play a major role as compared to extrinsic charge compensation.

These results highlight the unique information that can be obtained from EIS, in which separate circuit elements report on the state of the film, electrolyte, and redox-active probe as a function of temperature. It allows one to more fully describe the nature of transition, perhaps more so than simple calorimetry.

Our forthcoming work will integrate these results with simulations, which demonstrate that the origin of the polyelectrolyte's mobility upon heating through the transition is tied to rearrangement of water molecules on extrinsically compensated polyelectrolyte segments.

Acknowledgement

This material is based upon work supported by the National Science Foundation under Grant No. 1049706 and 1312676.

Notes and references

*Artie McFerrin Department of Chemical Engineering, Texas A&M University, College Station, Texas 77843,USA.
Email : jodie.lutkenhaus@tamu.edu

† Electronic Supplementary Information (ESI) available: [Bode plots; CPE, capacitance, and diffusion coefficient vs. tempearture; PSS amount in the film] See DOI: 10.1039/b000000x/

1. T. Boudou, T. Crouzier, K. F. Ren, G. Blin and C. Picart, *Adv. Mater.*, 2010, **22**, 441-467.
2. Y. Xiang, S. F. Lu and S. P. Jiang, *Chem. Soc. Rev.*, 2012, **41**, 7291-7321.
3. A. L. Becker, A. P. R. Johnston and F. Caruso, *Small*, 2010, **6**, 1836-1852.
4. G. Decher, *Science*, 1997, **277**, 1232-1237.
5. N. Malikova, I. Pastoriza-Santos, M. Schierhorn, N. A. Kotov and L. M. Liz-Marzan, *Langmuir*, 2002, **18**, 3694-3697.
6. D. Lee, D. Omolade, R. E. Cohen and M. F. Rubner, *Chem. Mat.*, 2007, **19**, 1427-1433.
7. G. Decher, B. Lehr, K. Lowack, Y. Lvov and J. Schmitt, 2nd CEC Workshop on Bioelectronics - Interfacing Biology with Electronics, Frankfurt, Germany, 1993.
8. R. von Klitzing, *Physical Chemistry Chemical Physics*, 2006, **8**, 5012-5033.
9. P. Lavalle, J. C. Voegel, D. Vautier, B. Senger, P. Schaaf and V. Ball, *Adv. Mater.*, 2011, **23**, 1191-1221.
10. K. Kohler, D. G. Shchukin, H. Mohwald and G. B. Sukhorukov, *J. Phys. Chem. B*, 2005, **109**, 18250-18259.
11. K. Kohler, H. Mohwald and G. B. Sukhorukov, *J. Phys. Chem. B*, 2006, **110**, 24002-24010.
12. C. Sung, A. Vidyasagar, K. Hearn and J. L. Lutkenhaus, *Journal of Materials Chemistry B*, 2014, **2**, 2088-2092.
13. P. Lavalle, C. Picart, J. Mutterer, C. Gergely, H. Reiss, J. C. Voegel, B. Senger and P. Schaaf, *J. Phys. Chem. B*, 2004, **108**, 635-648.
14. A. Vidyasagar, C. Sung, R. Gamble and J. L. Lutkenhaus, *ACS Nano*, 2012, **6**, 6174-6184.
15. R. Mueller, K. Kohler, R. Weinkamer, G. Sukhorukov and A. Fery, *Macromolecules*, 2005, **38**, 9766-9771.
16. B. Fortier-McGill and L. Reven, *Macromolecules*, 2009, **42**, 247-254.
17. A. Vidyasagar, C. Sung, K. Losensky and J. L. Lutkenhaus, *Macromolecules*, 2012, **45**, 9169-9176.
18. L. Shao and J. L. Lutkenhaus, *Soft Matter*, 2010, **6**, 3363-3369.
19. R. F. Shamoun, H. H. Hariri, R. A. Ghostine and J. B. Schlenoff, *Macromolecules*, 2012, **45**, 9759-9767.
20. R. Gabai, N. Sallacan, V. Chegel, T. Bourenko, E. Katz and I. Willner, *J. Phys. Chem. B*, 2001, **105**, 8196-8202.
21. J. H. Zhou, G. Wang, J. Q. Hu, X. B. Lu and J. H. Li, *Chem. Commun.*, 2006, 4820-4822.
22. H. Y. Lu and N. F. Hu, *J. Phys. Chem. B*, 2007, **111**, 1984-1993.
23. V. Pardo-Yissar, E. Katz, O. Lioubashevski and I. Willner, *Langmuir*, 2001, **17**, 1110-1118.
24. S. V. P. Barreira, V. Garcia-Morales, C. M. Pereira, J. A. Manzanares and F. Silva, *J. Phys. Chem. B*, 2004, **108**, 17973-17982.
25. T. R. Farhat and J. B. Schlenoff, *Langmuir*, 2001, **17**, 1184-1192.
26. T. R. Farhat and J. B. Schlenoff, *Journal of the American Chemical Society*, 2003, **125**, 4627-4636.

27. T. H. Silva, V. Garcia-Morales, C. Moura, J. A. Manzanares and F. Silva, *Langmuir*, 2005, **21**, 7461-7467.
28. T. Alonso-Garcia, M. J. Rodriguez-Presa, C. Gervasi, S. Moya and O. Azzaroni, *Anal. Chem.*, 2013, **85**, 6561-6565.
29. B. Schoeler, G. Kumaraswamy and F. Caruso, *Macromolecules*, 2002, **35**, 889-897.
30. J. J. Harris, J. L. Stair and M. L. Bruening, *Chem. Mat.*, 2000, **12**, 1941-1946.
31. J. J. Harris, P. M. DeRose and M. L. Bruening, *Journal of the American Chemical Society*, 1999, **121**, 1978-1979.
32. N. Gu, D. Wei, L. Niu and A. Ivaska, *Electrochimica Acta*, 2006, **51**, 6038-6044.
33. Q. C. Ruan, Y. C. Zhu, F. Li, J. W. Xiao, Y. Zeng and F. F. Xu, *Journal of Colloid and Interface Science*, 2009, **333**, 725-733.
34. A. Amirudin and D. Thierry, *Progress in Organic Coatings*, 1995, **26**, 1-28.
35. F. Zhou, H. Y. Hu, B. Yu, V. L. Osborne, W. T. S. Huck and W. M. Liu, *Anal. Chem.*, 2007, **79**, 176-182.
36. T. A. Garcia, C. A. Gervasi, M. J. R. Presa, J. I. Otamendi, S. E. Moya and O. Azzaroni, *Journal of Physical Chemistry C*, 2012, **116**, 13944-13953.
37. V. F. Lvovich, in *Impedance Spectroscopy*, John Wiley & Sons, Inc., 2012, pp. 37-47.
38. L. Krasemann and B. Tieke, *Langmuir*, 2000, **16**, 287-290.
39. Z. L. Cheng, L. Cheng, S. J. Dong and X. R. Yang, *J. Electrochem. Soc.*, 2001, **148**, E227-E232.
40. S. Umadevi, V. Ganesh and S. Berchmans, *RSC Advances*, 2014, **4**, 16409-16417.
41. R. A. Ghostine and J. B. Schlenoff, *Langmuir*, 2011, **27**, 8241-8247.
42. R. A. Ghostine, M. Z. Markarian and J. B. Schlenoff, *Journal of the American Chemical Society*, 2013, **135**, 7636-7646.
43. E. P. M. Vanwesting, G. M. Ferrari and J. H. W. Dewit, *Corrosion Sci.*, 1994, **36**, 979-994.
44. E. Frechette, C. Compere and E. Ghali, *Corrosion Sci.*, 1992, **33**, 1067-1081.
45. E. P. M. Vanwesting, G. M. Ferrari and J. H. W. Dewit, *Corrosion Sci.*, 1993, **34**, 1511-1530.
46. G. Inzelt and G. Lang, *Electrochimica Acta*, 1991, **36**, 1355-1361.
47. V. F. Lvovich, in *Impedance Spectroscopy*, John Wiley & Sons, Inc., 2012, pp. 59-96.
48. R. N. Vyas, K. Y. Li and B. Wang, *J. Phys. Chem. B*, 2010, **114**, 15818-15824.
49. E. Sabatani, J. Cohenboulakia, M. Bruening and I. Rubinstein, *Langmuir*, 1993, **9**, 2974-2981.
50. J. J. I. Ramos, S. Stahl, R. P. Richter and S. E. Moya, *Macromolecules*, 2010, **43**, 9063-9070.
51. S. Han and B. Lindholm-Sethson, *Electrochimica Acta*, 1999, **45**, 845-853.
52. L. L. Han, Z. W. Mao, H. Wuliyasu, J. D. Wu, X. Gong, Y. G. Yang and C. Y. Gao, *Langmuir*, 2012, **28**, 193-199.
53. C. Y. Gao, S. Leporatti, S. Moya, E. Donath and H. Mohwald, *Chem.-Eur. J.*, 2003, **9**, 915-920.
54. N. Ladhari, J. Hemmerle, C. Ringwald, Y. Haikel, J. C. Voegel, P. Schaaf and V. Ball, *Colloid Surf. A-Physicochem. Eng. Asp.*, 2008, **322**, 142-147.
55. R. A. McAloney, M. Sinyor, V. Dudnik and M. C. Goh, *Langmuir*, 2001, **17**, 6655-6663.
56. S. T. Dubas and J. B. Schlenoff, *Langmuir*, 2001, **17**, 7725-7727.
57. R. A. McAloney, V. Dudnik and M. C. Goh, *Langmuir*, 2003, **19**, 3947-3952.